X-ray absorption spectroscopy study of annealing process on Sr$_{1-x}$La$_x$CuO$_2$ electron-doped cuprate thin films

A. Galdi, P. Orgiani, C. Sacco, B. Gobaut, P. Torelli, C. Aruta, N. B. Brookes, M. Minola, J. W. Harter, K. M. Shen, D. G. Schlom, and L. Maritato

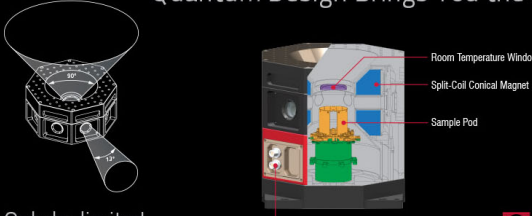**Articles you may be interested in**

Layer-by-layer shuttered molecular-beam epitaxial growth of superconducting Sr$_{1-x}$La$_x$CuO$_2$ thin films
Journal of Applied Physics **113**, 053911 (2013); 10.1063/1.4790150

X-ray absorption spectroscopy study of annealing process on Sr$_{1-x}$La$_x$CuO$_2$ electron-doped cuprate thin films

A. Galdi,[1,2,a)] P. Orgiani,[2] C. Sacco,[2,3] B. Gobaut,[4] P. Torelli,[5] C. Aruta,[6] N. B. Brookes,[7] M. Minola,[8,b)] J. W. Harter,[9] K. M. Shen,[9,10] D. G. Schlom,[10,11] and L. Maritato[2,3]

[1]*Dipartimento di Ingegneria dell'Informazione, Elettrica e Matematica Applicata, Università degli Studi di Salerno, I-84084 Fisciano, SA, Italy*
[2]*CNR-SPIN Salerno, Università degli Studi di Salerno, I-84084 Fisciano, SA, Italy*
[3]*Dipartimento di Ingegneria Industriale-DIIN, Università di Salerno, I-84084 Fisciano, SA, Italy*
[4]*Elettra Sincrotrone Trieste S.C.p.A., I-34149 Trieste, Italy*
[5]*CNR Istituto Officina dei Materiali, TASC National Laboratory, I-34149 Trieste, Italy*
[6]*CNR-SPIN, Università di Roma Tor Vergata, I-00133 Roma, Italy*
[7]*European Synchrotron Radiation Facility, F-38043 Grenoble Cedex, France*
[8]*CNR-SPIN and Dipartimento di Fisica, Politecnico di Milano, Piazza Leonardo Da Vinci 32, I-20133 Milano, Italy*
[9]*Laboratory of Atomic and Solid State Physics, Department of Physics, Cornell University, Ithaca, New York 14853, USA*
[10]*Kavli Institute for Nanoscale Science, Ithaca, New York 14853, USA*
[11]*Department of Materials Science and Engineering, Cornell University, Ithaca, New York 14853, USA*

The superconducting properties of Sr$_{1-x}$La$_x$CuO$_2$ thin films are strongly affected by sample preparation procedures, including the annealing step, which are not always well controlled. We have studied the evolution of Cu $L_{2,3}$ and O K edge x-ray absorption spectra (XAS) of Sr$_{1-x}$La$_x$CuO$_2$ thin films as a function of reducing annealing, both qualitatively and quantitatively. By using linearly polarized radiation, we are able to identify the signatures of the presence of apical oxygen in the as-grown sample and its gradual removal as a function of duration of 350 °C Ar annealing performed on the same sample. Even though the as-grown sample appears to be hole doped, we cannot identify the signature of the Zhang-Rice singlet in the O K XAS, and it is extremely unlikely that the interstitial excess oxygen can give rise to a superconducting or even a metallic ground state. XAS and x-ray linear dichroism analyses are, therefore, shown to be valuable tools to improving the control over the annealing process of electron doped superconductors. *Published by AIP Publishing.*
https://doi.org/10.1063/1.5021559

I. INTRODUCTION

Electron-doped (e-doped) cuprate superconductors have been extensively studied over the past decades, providing a useful point of comparison to the more abundant family of hole-doped (h-doped) cuprate high-temperature superconductors.[1] Recent studies on h-doped cuprates have tried to shed light on the mechanism of high-temperature superconductivity in these systems, identifying nematic phases, charge density waves,[2] paramagnons,[3] and non-Fermi liquid behavior.[4] It is natural to seek such phenomena in the electron doped counterpart,[1,5] in order to exclude the non-essential properties for high-temperature superconductivity to occur.

Among the cuprate superconductors, the infinite layer (IL) compound SrCuO$_2$ is the one with the simplest crystal structure that can be electron doped[6] by substituting a trivalent rare-earth cation for Sr. Remarkably, it is also the e-doped cuprate with the highest T_c ($\approx$40 K in bulk).[1] Its tetragonal structure is characterized by CuO$_2$ planes alternating with Sr planes, so that Cu coordination is purely square planar.[7] This system is particularly interesting because its simple structure does not involve charge reservoir blocks that, in e-doped compounds, often contain magnetic rare-earth ions.[8] In addition to fundamental studies, the simple crystal structure of IL cuprates makes them particularly suitable for the engineering of heterostructures or artificial superlattices. Examples are oxide-based ferromagnet-superconductor (F-S or F-S-F) junctions or (SrCuO$_2$)$_n$[(Ca/Ba)CuO$_2$]$_m$[9,10] superlattices.

It is well known that e-doped cuprates need an oxygen reduction step in order to become superconducting;[1,8,11] for the Sr$_{1-x}$La$_x$CuO$_2$ (SLCO) thin films investigated here, vacuum annealing is performed *in-situ* after growth.[12] What exactly occurs during the reduction process is still unclear; it is commonly accepted that it removes excess oxygen present at the Cu apical site (sites that are unoccupied in the e-doped cuprate structures, while apical oxygen is present in h-doped compounds).[1,11,13] In contrast to this notion, a transmission electron microscopy study of Nd$_{2-x}$Ce$_x$CuO$_4$ has revealed that other structural modifications occur,[14] involving the migration of Cu ions, while the amount of oxygen removed is usually very small[13] and close to the detection limit of many experimental methods. Moreover, experiments with higher sensitivity to oxygen removal, such as neutron

[a)]Present address: Cornell Laboratory for Accelerator-based Sciences and Education, Cornell University, Ithaca, New York 14853, USA. ag733@cornell.edu.
[b)]Present address: Max-Planck-Institut für Festkörperforschung, Heisenbergstrasse 1, D-70569 Stuttgart, Germany.

diffraction, are extremely difficult to perform on thin film samples.[1,8]

Here, we report a study on near edge x-ray absorption spectroscopy (XAS) measurements at Cu $L_{2,3}$ and O K edges on SLCO thin films with different post-growth treatments. The data reveal modifications to the Cu coordination and to the density of states (DOS) at the conduction band. These modifications can be ascribed to the presence of apical oxygen in the unreduced and partially reduced samples. The quantitative analysis of the Cu $L_{2,3}$ spectra shows that the excess oxygen causes the unreduced "as-grown" (nonsuperconducting) sample to be hole doped, but the O K edge spectra do not show the typical features observed in h-doped superconductors. We attribute this different behavior either to the strong perturbation of the Cu orbital occupation or to the disorder introduced by the interstitial oxygen ions.

II. EXPERIMENTAL

Epitaxial SLCO films ($x = 0$ to $x = 0.13$) were grown using shuttered layer-by-layer deposition in a reactive MBE system equipped with reflection high-energy electron diffraction (RHEED), as described in detail in Ref. 12. The state-of-the-art MBE growth technique allows the (Sr, La):Cu stoichiometry to be tuned with an accuracy of about 1%. The growth temperature ranged from 500 to 510 °C, and the background pressure of distilled O_3 during growth ranged from 3×10^{-7} to 1×10^{-6} Torr. The samples hereafter named "*in-situ* annealed" were annealed *in-situ* immediately after the growth in a vacuum at 10 °C above the growth temperature for 30 min. The annealing process has been optimized (in terms of temperature and duration) by monitoring the sample T_c and resistivity. During annealing, the samples were monitored by RHEED, following the evolution of a typical surface reconstruction.[15] The "as-grown" samples were cooled down in the distilled ozone of same pressure in which they were deposited.

The samples ranged from 45 to 120 unit cells in thickness and were grown on (110) oriented GdScO$_3$ and DyScO$_3$ substrates. These substrates have pseudo-cubic lattice constants of 0.397 nm and 0.394 nm, respectively, that stabilize the IL structure of SLCO (in-plane lattice parameter $a = 0.393$ nm for $x = 0$ and $a = 0.395$ nm for $x = 0.10$ in bulk samples).[6,17] All samples were characterized by x-ray diffraction, which showed that the films were (001) orientated and exhibited a constant out-of-plane lattice parameter (c-axis) as a function of film thickness.[12]

XAS spectra were measured on the ID08 beamline of the European Synchrotron Radiation Facility (Grenoble, France) at the Cu $L_{2,3}$ absorption edge and at the APE beamline of the Elettra synchrotron (Trieste, Italy) at Cu $L_{2,3}$ and O K edges. At the APE beamline, the as-grown samples were annealed at 350 °C in 1 Torr of Ar for times ranging from 5 to 20 min, using a chamber connected to the XAS measurement chamber; the XAS spectra of the samples were measured before and after each annealing step.

The absorption signal was measured by the fluorescence yield (FY) and the total electron yield (TEY) at the Cu absorption edge, and only by TEY at the O K absorption edge. We did not observe significant self-absorption effects

in the FY measurements when compared to TEY ones, probably because of the small sample thickness[16] and the nongrazing geometry of the outgoing x-ray beam which minimizes the path for self-absorption. The measured fluorescence and current signals have been normalized by the incident flux, as measured by the current from a mesh along the monochromatic beam path. XAS spectra were normalized by fitting a constant background before the absorption edge, then subtracting it from the data, and finally setting the intensity at a higher photon energy, far from the absorption edge, to unity. The measurements were performed using linearly polarized photons with the electric vector $\vec{E}$ either in the plane (H polarization) or perpendicular to the plane (V polarization) of the synchrotron orbit. At normal incidence, $\vec{E}$ lies in the sample plane for both polarizations, whereas at grazing incidence and H polarization (30° from the surface), $\vec{E}$ is nearly parallel to the c–axis of the samples. In this way, the absorption spectra with $\vec{E} \perp c$ and $\vec{E} \| c$ and the corresponding x-ray linear dichroism (XLD) can be measured. Following convention, we define

$$\begin{aligned} \text{XLD} &= \text{XAS}(\vec{E} \perp c) - \text{XAS}(\vec{E} \| c) \\ &\propto \text{XAS}(V, 30°) - \text{XAS}(H, 30°), \end{aligned} \tag{1}$$

or equivalently by using XAS(H, 90°) in place of XAS(V, 30°). XLD is sensitive to the axial anisotropy of the electron DOS; in this case, induced by orbital occupation of the Cu $3d$ states. Indeed, with $\vec{E} \| c$, transition to states mainly originating from out-of-plane orbitals determines the absorption signal (such as Cu $3d_{3z^2 - r^2}$ or O $2p_z$), while those originating from in-plane orbitals are probed with $\vec{E} \perp c$ (such as Cu $3d_{x^2 - y^2}$ or O $2p_{x,y}$).

For the quantitative analysis of the XAS spectra, the isotropic absorption spectrum has been obtained as

$$\text{XAS}_{\text{ISO}} = \text{XAS}(V, 30°)(1 - \tan^2(30°)) + \frac{\text{XAS}(H, 30°)}{\cos^2(30°)}, \tag{2}$$

or equivalently by using XAS(H, 90°) in place of XAS(V, 30°).

III. RESULTS

A. Cu L_3 edge absorption spectra

Figures 1(a)–1(d) show the Cu L_3 XAS$_{\text{ISO}}$ spectra of a series of *in-situ* annealed SLCO samples with different doping concentrations, after background subtraction. The series of samples exhibits all of the typical features we observed in the XAS spectra of SLCO. The high-resolution spectra were collected at the European Synchrotron Radiation Facility. The sample series was grown at 510 °C under a background partial pressure of 1×10^{-6} Torr O$_3$.

As the majority of Cu ions in SLCO are in the 2+ oxidation state, strong absorption is expected at a photon energy $E = 931.4$ eV, corresponding to the $3d^9 \rightarrow \underline{2p}3d^{10}$ transition (here, $\underline{2p}$ represents a hole in the $2p$ core level). Together with this peak, Cu^{2+} is characterized by a weaker peak at $E \approx 936$ eV, corresponding to the transition to the $\underline{2p}3d^9 4s$ final state.[18] Upon electron doping, a peak at $E \approx 93\overline{4}$ eV has
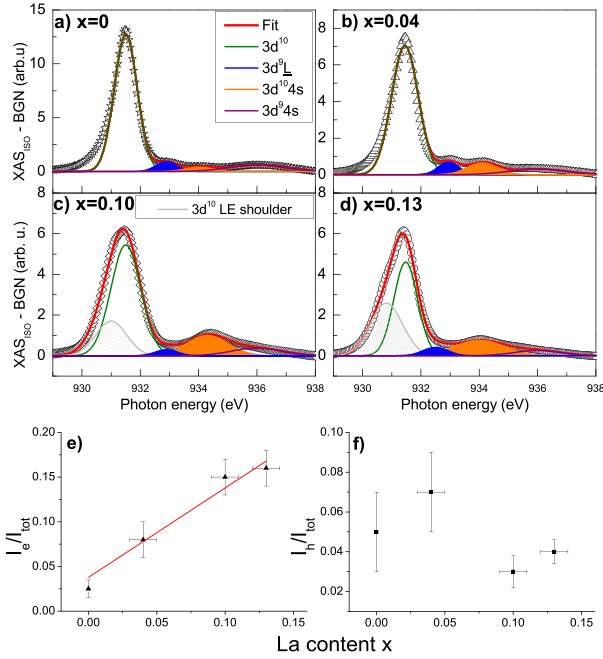
FIG. 1. (a)–(d) L_3 edge of *in-situ* annealed SLCO samples with different doping levels (symbols) and fits of the XAS$_{ISO}$ spectra with 4 or 5 Gaussian curves [panels (a)–(b) and (c)–(d), respectively] centered at fixed energy values, corresponding to the transition energies reported in the text (lines). A first-order Shirley background has been subtracted from all spectra. In the labels, the final (excited) $3d$ states are indicated. (e) Relative intensity (area) of the peak associated with doped electrons (orange) and (f) relative intensity of the peak associated with holes (blue), as a function of La content x.

been reported in SLCO, that can be attributed to the $Cu^{1+} \, 3d^{10} \rightarrow \underline{2p}3d^{10}4s$ transition.[18,20] States arising from hole introduction, instead, have a predominant $3d^9\underline{L}$ character (where $\underline{L}$ represents a hole in the oxygen ligand orbital), and the corresponding absorption peak $(3d^9\underline{L} \rightarrow \underline{2p}3d^{10}\underline{L})$ is at $E \approx 932.9 \, eV$. Such hole-related states have been reported for hole doped cuprates[21] and apical-oxygen-rich IL compounds such as $BaCuO_{2+x}$.[22] A scheme of transitions is reported in Fig. S1 of the supplementary materials. According to this, the spectra have been decomposed with a series of Gaussian peaks, corresponding to transitions to the Cu $3d$–$4s$ excited states, using the fitting procedure described in detail in the supplementary materials.

For some of the samples of the series [see Figs. 1(c) and 1(d)], we observed that the main peak is split into two components; we then added an additional low energy (LE) component 0.4–0.5 eV below the Cu^{2+} peak. A peak at this energy was already reported in the XAS measurements of cuprate-manganite interfaces,[23,24] and the authors interpreted it as originating from a modification of Cu coordination/orbital occupation (in particular, occurring at the interfaces), rather than valence modification.

In Figs. 1(e) and 1(f), we report the area of the Cu^{1+} (I_e) and hole (I_h) related peaks, normalized to the total area, I_{tot}, as a function of nominal doping. The quantity I_e/I_{tot} is expected to increase linearly with doping in e-doped cuprates,[18,19] since it represents the fraction of Cu in the $1+$ valence state. Data shown in Fig. 1(e) are in good agreement with a line of slope 1 with a non-zero intercept, within the experimental error associated with the La content

(± 0.01)[12] and the error associated with I_e/I_{tot} from the fitting of the spectra.

In hole-doped cuprates, I_h/I_{tot} is shown to scale linearly with hole content,[19,21] at least up to 10% doping. Figure 1(f) suggests that a small amount of hole states ($\lesssim$7%) is present in the samples of the series.

The Cu coordination in IL cuprates is square planar, resulting in a strong orbital polarization of Cu^{2+} that leaves the $3d_{x^2-y^2}$ orbital unoccupied (see Fig. S1 of the supplementary materials). This results in a strong positive XLD that is typical of cuprate compounds.[21] In Fig. 2(b), we report the normalized XLD spectra of the same series of samples as Fig. 1, while the isotropic XAS spectra are reported in Fig. 2(a) for reference. It is interesting to note that the e-doping related peak at 934 eV does not contribute to XLD due to the spherical symmetry of the final state ($\underline{2p}3d^{10}4s$). On the other hand, in the samples with $x = 0$, 0.04, characterized by a higher I_h/I_{tot} value, a positive linear dichroism is associated with the 932.9 eV peak. This finding is in agreement with XLD measurements on hole-doped cuprates[21] and hole-doped IL-based heterostructures,[22,25] confirming the attribution of the peak at 932.9 eV to holes.

For the samples showing splitting of the Cu^{2+} peak in the LE component ($x = 0.10$ and 0.13), a suppression of XLD intensity on the left of the Cu^{2+} peak is observed, as is evident from Fig. 2(b).

B. Effect of annealing and O *K* edge absorption

In Fig. 3(a), the XAS spectra of two SLCO ($x = 0.1$) samples, grown sequentially under the same conditions, are
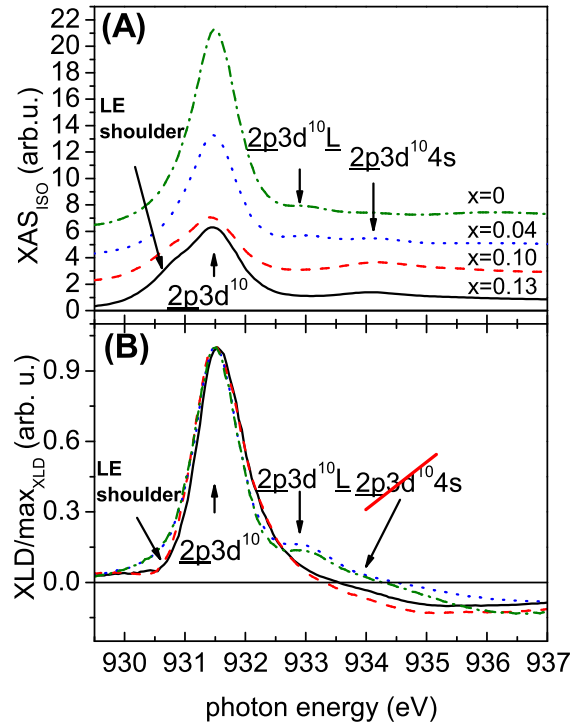

FIG. 2. (a) Isotropic XAS spectra and (b) normalized XLD spectra of the same *in-situ* annealed sample series as Fig. 1. XLD spectra are normalized by their maximum. When the LE shoulder component is present ($x = 0.10$, 0.13), a reduction of the XLD signal is observed.
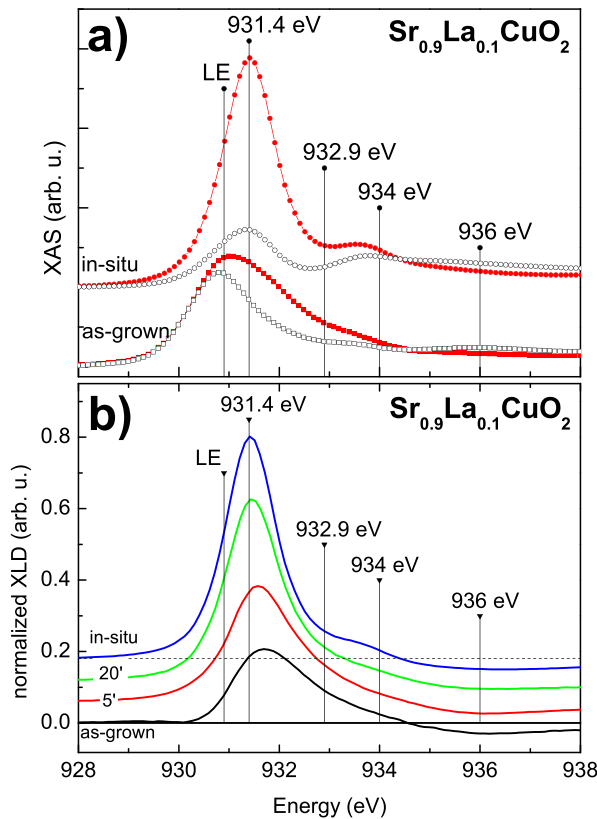
FIG. 3. (a) XAS Cu L_3 spectra measured with H polarization and at incident angles of 90° (red filled symbols) and 30° (black hollow symbols) of the as-grown and *in-situ* annealed $x = 0.1$ samples. (b) Normalized XLD Cu L_3 spectra of the as-grown, 5′-Ar annealed, 20′-Ar annealed and *in-situ* annealed $x = 0.1$ samples. The XLD is normalized to the maximum of the corresponding XAS_{ISO} spectrum. The energy positions of the spectral components, previously used to decompose the XAS_{ISO} spectra, are indicated by the vertical lines. The spectra are vertically shifted for clarity, by adding a constant offset value.

shown. The samples have been grown on $DyScO_3$ substrates with a background pressure of 3×10^{-7} Torr of O_3 and with a substrate temperature of 500 °C. The 510 °C *in-situ* annealed sample is superconducting with $T_c = 33$ K. Details on the structural and transport properties of samples as a function of *in-situ* annealing are reported in the supplementary materials.

The *in-situ* annealed sample is characterized by a dominant peak corresponding to Cu^{2+} characterized by a strong dichroism. The peak close to 934 eV can be attributed mainly to e-doping. On the other hand, the dominant peak in the as-grown sample spectra is found at 930.9 eV, corresponding to the energy of the LE shoulder observed in Fig. 1. The corresponding XLD spectra, normalized to the maximum of isotropic XAS spectrum, of the annealed and as-grown samples are reported in Fig. 3(b). The maximum XLD is found at the same energy as the XAS maximum (i.e., 931.4 eV) for the *in-situ* annealed sample. For the as-grown sample, the main XAS peak does not contribute to XLD, and the XLD maximum is found at a higher energy (about 931.7 eV) and the overall intensity is strongly reduced. The XLD peak is broader for the as-grown sample than the *in-situ* annealed one. In particular, we can observe a broad positive XLD extending beyond 934 eV. As oxygen is removed from the as-grown samples by annealing for 5 and 20 min at 350 °C in
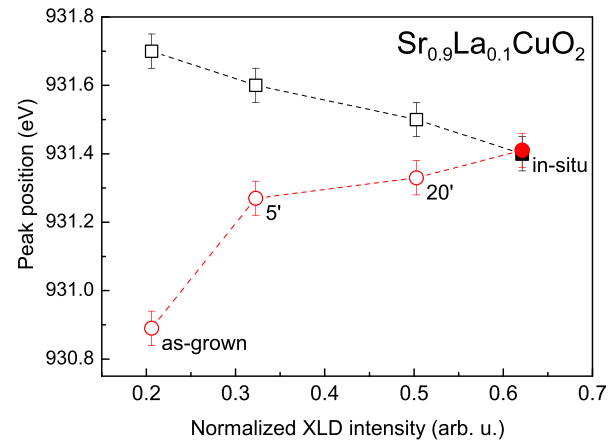

FIG. 4. Position of the maximum of Cu L_3 XAS_{ISO} (circles) and XLD (squares) plotted versus the normalized XLD intensity maximum. Open symbols represent the as-grown sample as deposited (labelled as-grown) and after 5′- and 20′-annealing at 350 °C in Ar; filled symbols represent the 510 °C *in-situ* annealed sample. The dashed lines are guide to the eye.

Ar, the XLD spectra evolve by an increased intensity, reduced broadening and a shift of the maximum to a lower energy. The evolution of the XAS_{ISO} and XLD maximum energy (on the vertical axis) and XLD intensity (on the horizontal axis) is resumed in Fig. 4. The maximum of the isotropic spectra in the oxygen rich samples is found at lower energy than the *in-situ* annealed one, while the XLD maximum exhibits the opposite behavior, due to different anisotropy properties of the two observed Cu^{2+} components. For the *in-situ* annealed sample, where we assume that all the Cu^{2+} ions are in the expected square planar coordination, the maxima of the XAS_{ISO} and XLD spectra are coincident.

In Fig. 5, we report the oxygen K edge spectra of the *in-situ* annealed and as-grown samples. Red filled and black hollow symbols represent the absorption for $\vec{E} \perp c$ and $\vec{E} \parallel c$, respectively. The O K edge XAS corresponds to the $1s \rightarrow 2p$ transition; its intensity is closely related to the O $2p$ partial DOS, that is crucial for the properties of cuprate superconductors. Indeed, thanks to the hybridization of oxygen with the
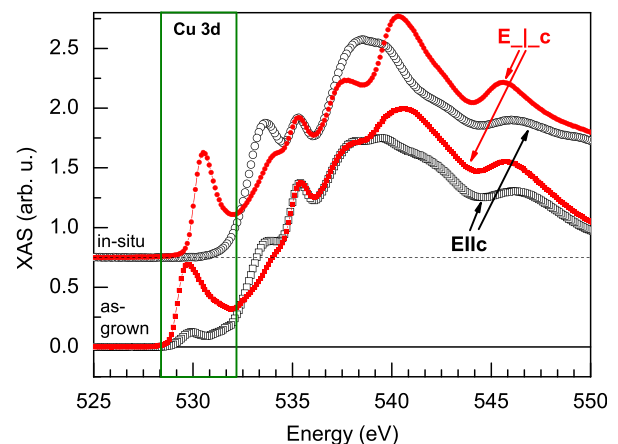

FIG. 5. Comparison of O K edge XAS spectra of as-grown (squares) and 510 °C *in-situ* annealed $x = 0.1$ samples (circles). The spectra have been measured with H polarized radiation. The red filled symbols represent the XAS with the electric field perpendicular to the c-axis of the samples, while the black hollow symbols represent the XAS with the electric field parallel to c. The spectra are vertically shifted for clarity.

Cu, Sr and La ions, the O $2p$ partial DOS reflects the features of the unoccupied metal states, providing complementary information about the electronic structure of the films.[26]

The data in Fig. 5 clearly show increased dichroism in the *in-situ* annealed sample compared to the as-grown one. This is particularly relevant in the pre-edge region, associated with the hybridization of oxygen with the Cu 3d states. A characteristic feature of e-doped cuprates is that the pre-edge is only detected with $\vec{E} \perp c$ as a consequence of Cu orbital occupation and of Cu-O hybridization in plane (with O $2p_{x,y}$ orbitals).[21] Further evidence of this behavior is seen in Fig. 6(a), where the O K pre-edge is shown for the as-grown sample. The non-zero absorption for $\vec{E} \| c$ can be attributed to the presence of apical oxygen holes. Apical oxygen states are detected at the O K edge of several superconducting hole doped cuprate compounds, and are believed to play an important role in superconductivity.[27–30] In particular, the pre-edge peaks in hole doped cuprates for $\vec{E} \| c$ are found at a lower energy than the $\vec{E} \perp c$ features, since the O 1s level has a smaller binding energy for the apical oxygen. Conversely, for the IL as-grown sample, the pre-edge is found at higher energies for $\vec{E} \| \mathbf{c}$ ($\Delta_{AP} \approx 0.2$ eV).

In Fig. 6(b), we show the XLD at the O K pre-edge for the as-grown, 350 °C Ar annealed and 510 °C *in-situ* annealed samples. The pre-edge peak of the as-grown sample
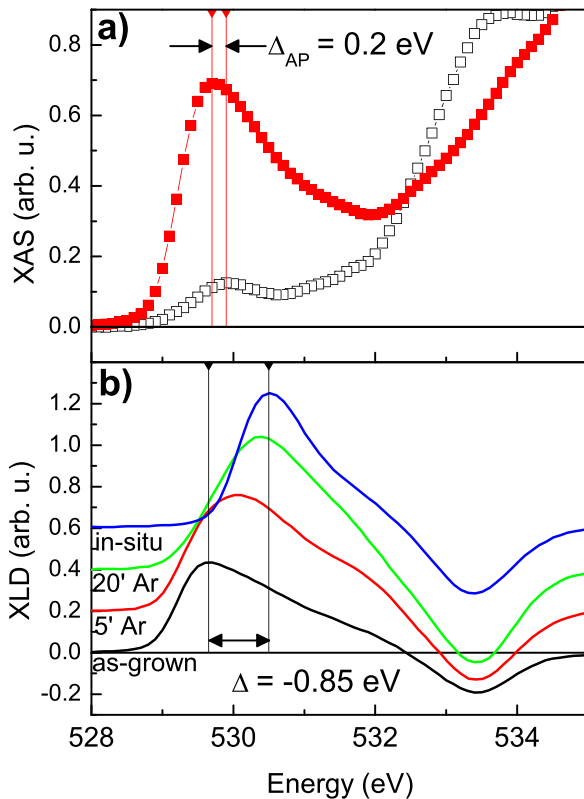
is found at 0.85 eV below the pre-edge of the *in-situ* annealed one. As oxygen is removed from the as-grown sample by Ar annealing, the peak shifts towards the position of the *in-situ* annealed one. At the same time, the corresponding XLD intensity also increases.

IV. DISCUSSION

By comparing the XAS spectra of *in-situ* annealed and as-grown samples, we observe that excess oxygen strongly perturbs the square planar coordination of Cu ions. While contributing to the structural distortion, oxygen excess also increases the Cu valence in the infinite layer compound (i.e., drains electrons and introduces holes) in order to balance charges.

The effect of excess oxygen on Cu coordination is revealed by comparing the XAS and XLD spectra of the *in-situ* annealed and as-grown samples in Fig. 3. The normalized XLD intensity in the as-grown sample is smaller by a factor of 3 with respect to the *in-situ* annealed one. Another signature of perturbation of the square planar coordination is that the main L_3 peak appears at lower energies in the as-grown sample than in the *in-situ* annealed one (see, for example, Fig. 4). This is evident in Fig. 7, where we report the fit of the XAS$_{ISO}$ spectra of the as-grown (a) and *in-situ* annealed (b) samples, following the same procedure used for the spectra shown in Fig. 2. For the as-grown sample, 77% of the spectral weight corresponding to the Cu^{2+} 3$d^9 \rightarrow 2p3d^{10}$ transition is transferred to the LE component. As shown in Figs. 2 and 3(b), the LE peak does not contribute to XLD, showing that it originates from Cu sites characterized by isotropic 3d orbital occupation, which we identify with Cu sites where apical oxygen is present.

The intensity corresponding to the 3$d^9\underline{L}$ in the fit of Fig. 7(a) reveals that in the as-grown sample, there is a large

FIG. 6. (a) Pre-edge region of the O K edge spectrum of the $x = 0.1$ as-grown sample. Red filled symbols represent the XAS with $\vec{E} \perp c$ and black hollow symbols with $\vec{E} \| c$. The vertical lines show the position of the pre-edge maxima in two different geometries. (b) XLD spectra of the O K pre-edge region of as-grown, 350 °C Ar annealed, and 510 °C *in-situ* annealed $x = 0.1$ samples. The spectra are vertically shifted for clarity. A shift in the pre-edge energy (Δ) of the as-grown samples with respect to the *in-situ* annealed one is evident.
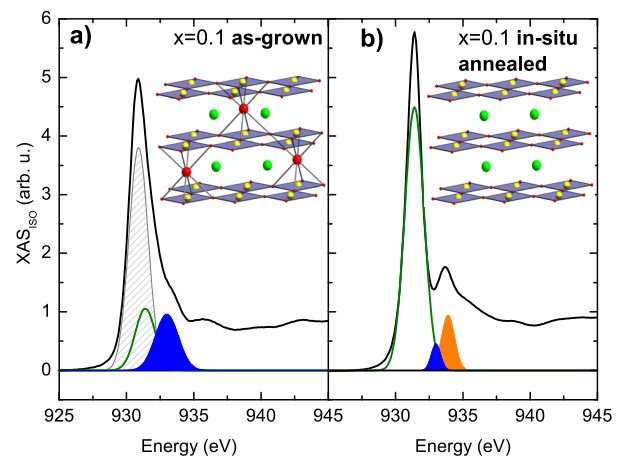

FIG. 7. Isotropic Cu L_3 XAS spectra of (a) the as-grown sample and (b) the *in-situ* annealed sample and their decomposition, following the procedure described in supplementary materials. The black line represents the XAS data, the light grey line the LE (at 930.9 eV), the green line the Cu^{2+} (at 931.4 eV), the blue filled peak the 3$d^9\underline{L}$, and the orange filled peak the Cu^{1+} components. The 936 eV component is not shown. In the inset, we report a sketch of the proposed crystal structure of the (a) as-grown (with oxygen randomly occupying the apical site) and (b) *in-situ* annealed (ideal IL structure) samples. Red spheres represent O, yellow spheres represent Cu and green spheres represent Sr/La.

density of holes that are introduced by excess oxygen ($I_h/I_{tot} = 0.20 \pm 0.07$). At the same time, within the resolution of our measurements, we are not able to detect the Cu^{1+} (e-doping) related peak in the as-grown sample. The fit results indicate that the hole component in the as-grown sample is broader than the one observed in the *in-situ* annealed sample, shown in Fig. 7(b), where we can attribute it to some residual holes induced by defects arising from a small Sr:Cu non-stoichiometry. This is in agreement with the observation that the XLD of the as-grown sample [shown in Fig. 3(b)] does not show a definite contribution at 932.9 eV, but rather a broad positive tail.

The resistivity versus temperature curve of the as-grown samples, reported in Fig. S3 of the supplementary materials, shows that the sample is metallic down to ≈ 80 K and becomes insulating at lower temperatures, even though no electron carriers are revealed by Cu XAS. We thus attribute the electrical conduction in the as-grown sample to hole carriers.

The O K edge XAS reveals noticeable differences between the as-grown sample and the typical XAS of the h-doped cuprates, despite the presence of hole carriers. The O K pre-edge of undoped cuprates originates from Cu 3d states forming the upper Hubbard band (UHB) at half filling. In e-doped cuprates (both of IL and T' structures), the O K pre-edge is found to be independent of doping.[21,28] Conversely, a strong dependence is found in the h-doped case: as holes are introduced, the spectral weight is removed from the UHB feature and transferred at a lower energy to the Zhang-Rice singlet state, which is observed at the O K edge ≈ -1.5 eV from the UHB.[21] In our case, we are not able to decompose the oxygen pre-edge into two distinct components but, as shown in Fig. 6(b), the pre-edge maximum of the as-grown sample is found at $\Delta = -0.85$ eV below that of the *in-situ* annealed one, and by partially removing oxygen via Ar annealing, the pre-edge maximum shifts towards the as-grown energy. This different behavior is related either to the strong perturbation of the orbital occupation of Cu ions, which is essential to the formation of the Zhang-Rice singlet,[32] or to the structural disorder induced by randomly distributed apical oxygen ions (see XRD data reported in Fig. S2 of the supplementary materials), which can be the source of the observed insulator-to-metal transition observed at 80 K in the as-grown sample.

The presence of apical oxygen holes is revealed by the $\vec{E} \| c$ pre-edge XAS, shown in Fig. 6, and the shift in pre-edge maxima for $\vec{E} \perp c$ and $\vec{E} \| c$ is $\Delta_{AP} > 0$, opposite to what is typically observed in h-doped cuprates.[27–29,31] In unreduced IL samples, the out-of-plane/in-plane lattice parameter ratio is smaller than one,[11,12] so that the Cu–O distance is expected to be smaller for the interstitial apical oxygen than for the in-plane one, while the opposite situation is realized for apical oxygen in h-doped cuprate structures. Several works have suggested that too strong hybridization of Cu states with the apical oxygen can destabilize the formation of the Zhang-Rice singlet state,[30,32–34] and this may be indeed the case for the as-grown sample.

V. CONCLUSIONS

We have studied the evolution of Cu $L_{2,3}$ and O K edge spectra of IL cuprate superconductors as a function of reducing annealing, both qualitatively and quantitatively. We identify from the XLD at Cu $L_{2,3}$ the signature of the presence of apical oxygen in the as-grown sample. The observation is confirmed by the measurements at the O K edge. Even though the as-grown sample appears to be hole doped, we cannot identify the signature of the Zhang-Rice singlet in the O K XAS, and it is extremely unlikely that the interstitial excess oxygen can give rise to a superconducting or even metallic ground state.

The modification of the XAS and XLD of the as-grown sample as a function of duration of 350 °C Ar annealing and the comparison with the *in-situ* annealed sample allow us to follow the process of gradual removal of the apical oxygen during the annealing process.

Given that the IL structure can be considered as the simplest realization of a cuprate superconductor, the present XAS and XLD data will be a useful reference for future studies of more complex systems, such as other T' e-doped cuprates and/or artificial heterostructures[5,23–25] based on different cuprate families.

SUPPLEMENTARY MATERIAL

See supplementary materials for Scheme of transitions at the Cu absorption edge; Fitting procedure at the Cu absorption edge; Properties of the as-grown and *in-situ* annealed samples.

ACKNOWLEDGMENTS

[1] N. P. Armitage, P. Fournier, and R. L. Greene, Rev. Mod. Phys. **82**, 2421 (2010).

[2] M. H. Fischer, S. Wu, M. Lawler, A. Paramekanti, and E. Kim, New J. Phys. **16**, 093057 (2014).

[3] M. Le Tacon, G. Ghiringhelli, J. Chaloupka, M. Moretti Sala, V. Hinkov, M. W. Haverkort, M. Minola, M. Bakr, K. J. Zhou, S. Blanco-Canosa, C. Monney, Y. T. Song, G. L. Sun, C. T. Lin, G. M. De Luca, M. Salluzzo, G. Khaliullin, T. Schmitt, L. Braicovich, and B. Keimer, Nat. Phys. **7**, 725–730 (2011).

[4] T. Das, R. S. Markievicz, and A. Bansil, Phys. Rev. B **81**, 184515 (2010).

[5] G. Dellea, M. Minola, A. Galdi, D. Di Castro, C. Aruta, N. B. Brookes, C. J. Jia, C. Mazzoli, M. Moretti Sala, B. Moritz, P. Orgiani, D. G. Schlom, A. Tebano, G. Balestrino, L. Braicovich, T. P. Devereaux, L. Maritato, and G. Ghiringhelli, Phys. Rev. B **96**, 115117 (2017).

[6] M. G. Smith, A. Manthiram, J. Zhou, J. B. Goodenough, and J. T. Markert, Nature **351**, 549 (1991).

[7]J. D. Jorgensen, P. G. Radaelli, D. G. Hinks, J. L. Wagner, S. Kikkawa, G. Er, and F. Kanamaru, Phys. Rev. B **47**, 14654(R) (1993).

[8]P. Fournier, Physica C **514**, 314 (2015).

[9]C. Aruta, G. Balestrino, S. Desfeux, S. Martellucci, and A. Paoletti, Appl. Phys. Lett. **68**, 926 (1996).

[10]D. P. Norton, B. C. Chakoumakos, D. H. Lowndes, and J. D. Budai, Appl. Surf. Sci. **96–98**, 672 (1996).

[11]Z. Z. Li, V. Jovanovich, H. Raffy, and S. Megtert, Physica C **469**, 73 (2009).

[12]L. Maritato, A. Galdi, P. Orgiani, J. W. Harter, J. Schubert, K. M. Shen, and D. G. Schlom, J. Appl. Phys. **113**, 053911 (2013).

[13]T. Adachi, Y. Mori, A. Takahashi, M. Kato, T. Nishizaki, T. Sasaki, N. Kobayashi, and Y. Koike, J. Phys. Soc. Jpn. **82**, 063713 (2013).

[14]P. K. Mang, S. Larochelle, A. Mehta, O. P. Vajk, A. S. Erickson, L. Lu, W. J. L. Buyers, A. F. Marshall, K. Prokes, and M. Greven, Phys. Rev. B **70**, 094507 (2004).

[15]J. W. Harter, L. Maritato, D. E. Shai, E. J. Monkman, Y. Nie, D. G. Schlom, and K. M. Shen, Phys. Rev. B **92**, 035149 (2015).

[16]R. Carboni, S. Giovannini, G. Antonioli, and F. Boscherini, Phys. Scr. **2005**, 986–988 (2003).

[17]G. Er, F. Miyamoto, F. Kanamaru, and S. Kikkawa, Physica C **181**, 206 (1991).

[18]Y. Tanaka, M. Karppinen, J. Lee, R. Liu, J. Chen, and H. Yamauchi, Solid State Commun. **147**, 370 (2008).

[19]Y. Tanaka, M. Karppinen, T. Kobayashi, T. S. Chan, R. S. Liu, J. M. Chen, and H. Yamauchi, Chem. Mater. **20**, 5414–5420 (2008).

[20]R. S. Liu, J. M. Chen, P. Nachimuthu, R. Gundakaram, C. U. Jung, J. Y. Kim, and S. I. Lee, Solid State Commun. **118**, 367 (2001).

[21]J. Fink, N. Nucker, E. Pellegrin, H. Romberg, and M. Knupfer, J. Electron Spectrosc. Relat. Phenom. **66**, 395 (1994).

[22]C. Aruta, G. Ghiringhelli, C. Dallera, F. Fracassi, P. G. Medaglia, A. Tebano, N. B. Brookes, L. Braicovich, and G. Balestrino, Phys. Rev. B **78**, 205120 (2008).

[23]J. Chakhalian, W. J. Freeland, H. U. Habermeier, G. Cristiani, G. Khaliullin, M. van Veenendaal, and B. Keimer, Science **318**, 1114 (2007).

[24]N. Yang, D. Di Castro, C. Aruta, C. Mazzoli, M. Minola, N. B. Brookes, M. Moretti Sala, W. Prellier, O. Lebedev, A. Tebano, and G. Balestrino, J. Appl. Phys. **112**, 123901 (2012).

[25]D. Di Castro, C. Aruta, A. Tebano, D. Innocenti, M. Minola, M. Moretti Sala, W. Prellier, O. Lebedev, and G. Balestrino, Supercond. Sci. Technol. **21**, 044016 (2014).

[26]M. Grioni, M. T. Czyzyk, F. M. F. de Groot, J. C. Fuggle, and B. E. Watts, Phys. Rev. B **39**, 4886 (1989).

[27]C. T. Chen, L. H. Tjeng, J. Kwo, H. L. Kao, P. Rudolf, F. Sette, and R. M. Fleming, Phys. Rev. Lett **68**, 2543 (1992).

[28]N. Nücker, M. Merz, P. Schweiss, E. Pellegrin, S. Schuppler, T. Wolf, V. Chakarian, Y. U. Idzerda, M. Kläser, G. Müller-Vogt, G. Er, S. Kikkawa, and G. Liu, J. Supercond. **12**, 143 (1999).

[29]P. Strivastava, B. R. Sekhar, C. Gasser, F. Studer, K. B. Garg, C. T. Chen, and M. Pompa, J. Phys.: Condens. Matter **10**, 3417 (1998).

[30]C. Di Castro, L. F. Feiner, and M. Grilli, Phys. Rev. Lett. **66**, 3209 (1991).

[31]M. Salluzzo, G. Ghiringhelli, N. B. Brookes, G. M. De Luca, F. Fracassi, and R. Vaglio, Phys. Rev. B **75**, 054519 (2007).

[32]F. C. Zhang and T. M. Rice, Phys. Rev. B **37**, 3759(R) (1988).

[33]Y. Ohta, T. Tohyama, and S. Maekawa, Phys. Rev. B **43**, 2968 (1991).

[34]D. Meyers, M. Swarnakamal, J.-G. Cheng, S. Middey, J.-S. Zhou, J. B. Goodenough, B. A. Gray, J. W. Freeland, T. Saha-Dasgupta, and J. Chakhalian, Sci. Rep. **3**, 1834 (2013).